

# SIMULATION OF THE ROTATIONAL SUBLVELS OF THE GROUND AND THE FIRST EXCITED VIBRATIONAL STATES OF H<sub>2</sub>S USING RESUMMATION METHODS

O. V. Naumenko, E. R. Polovtseva, A.D. Bykov

V.E. Zuev Institute of Atmospheric Optics, SB RAS, 1, Academician Zuev Square, Tomsk  
634021, Russia

## ABSTRACT

The rotational sublevels of the key (000) and (010) vibrational states of the H<sub>2</sub>S molecule were modeled with an accuracy close to experimental uncertainty using the generating function and Euler approaches. The predictive ability of the Hamiltonian's parameters derived is tested against variational calculations. Comparison of transitions wavenumbers obtained from the presently calculated set of the H<sub>2</sub>S (000) and (010) energy levels with simulated (000)-(000), (010)-(010) transitions included in HITRAN 2916 database revealed a large discrepancy up to 44 cm<sup>-1</sup>. Large sets of accurate rotational sublevels of the (000) and (010) states are calculated.

## I. INTRODUCTION

The ground (000) and first excited (010) are the key vibrational states of the H<sub>2</sub>S molecule, as majority of the observed rotational - vibrational transitions in absorption originate from the rotational sublevels of these states. The experimental energy levels of the lower vibrational state are preferably used to determine the upper level of transition. However, the experimental rotational energy levels of the H<sub>2</sub>S ground vibrational state were not available until recently [1]. In Ref. [1] a set of consistent experimental energy levels was derived from simultaneous consideration of the observed rovibrational transitions of H<sub>2</sub>S molecule. The accuracy of the energy level determination in [1] depends on the accuracy of transitions involving this level, and in case of a lack of input data or their inconsistency, the resulted level may be considerably distorted. On the other hand, the set of experimental energy levels [1] is limited in  $J$  and  $K_a$  rotational quantum numbers. Then, an accurate simulation could support the energy levels values [1], or even improve them by rejecting less accurate transition involved in level determination. In this contribution an accurate set of calculated (000) and (010) rotational energy levels is obtained for the H<sub>2</sub>S molecule from the fitting to the observed energy levels [1] using the effective rotational Hamiltonian based on different resummation methods of the divergent perturbation series.

## II. EFFECTIVE HAMILTONIAN AND ENERGY LEVELS FITTING

The rotational Hamiltonian written through the generating function  $G$  [2] has the form:

$$H_{rot}^G = \sum_{n,m} g_{nm} J^{2n} \left\{ G(\alpha^{(J)}) \right\}^m + \sum_{n,m} u_{nm} J^{2n} I(J_+^2 + J_-^2), \left\{ G(\alpha^{(J)}) \right\}^m J_+, \quad (1)$$

Where the generating function is defined according to [3]

$$G(\alpha^{(J)}) = (2/\alpha^{(J)}) \left\{ \sqrt{1 + \alpha^{(J)} J_z^2} - 1 \right\}.$$

The  $J$ -dependence of  $\alpha^{(J)}$  in the generating function is given by the development

$$\alpha^{(J)} = \sum_n \alpha_n J^{2n}.$$

Numerical parameters  $g_{nm}$ ,  $u_{nm}$ , and  $\alpha_n$  of Hamiltonian (1) are adjustable spectroscopic parameters. This representation of the rotational operator doesn't contain divergent series essential for the conventional perturbative approach, and proved to be much more accurate not only in the fitting, but also in the extrapolation calculations. Relations of the  $H_{rot}^G$  parameters with Watson's constants are discussed in [4]. Spectroscopic parameters of Hamiltonian (1) were determined in a least square fit to experimental rotational energies of each vibrational state.

Experimental energy levels derived in recent paper [1] for the (000) and (010) state of the H<sub>2</sub>S molecule were introduced into the least squares fitting using the effective Hamiltonian (1). The resulting parameters with 1 sigma confidential intervals are shown in Table 1. An RMS deviations on the order of 0.0002 cm<sup>-1</sup> what is close to experimental accuracy were obtained by varying of 37 and 35 parameters of Hamiltonian (1) for the (000) and (010) states, respectively.

In fact, we used Watson Hamiltonian, Pade-Borel approximants, generating functions (GF), and Euler resummation ( Ref. [6]) in the energy levels calculation. It seems that the GF approach provides most accurate fitting and extrapolation, that is why we show the illustrations which, mainly, concern only this method. To compare our results with the literature, we calculate large sets of the 000 and 010 energy levels and constructed pure rotational (000)-(000) and (010)-(010) transitions. Then these transitions were compared with the HITRAN 2016 data.

### **III. COMPARISON WITH THE HITRAN 2016 DATABASE AND VARIATIONAL CALCULATIONS**

HITRAN 2016 database contains both pure experimental and simulated pure rotational transition of H<sub>2</sub>S between 0 and 610 cm<sup>-1</sup>. These transitions are taken, mostly, from Ref. [5], where the experimental H<sub>2</sub>S spectra between 40 and 360 cm<sup>-1</sup> were assigned and modeled using Pickett program suite [6] which offers also the Euler resummation method. In the fitting in [5]

not only new experimental data were used, but all available information from the literature was included. The resulting list includes together with experimental transitions a large number of simulated frequencies, mostly for weak lines, with estimated accuracy on positions up to  $0.033\text{ cm}^{-1}$ .

The pure rotational (000)-(000) and (010)-(010) transitions of  $\text{H}_2\text{S}$  between 45 and  $360\text{ cm}^{-1}$  included into HITRAN data base were compared with those calculated based on parameters derived in this study. The comparison is included into Figs. 1-2 and Tables 2-3. It seen from Figs. **1 and 2** that there are large (up to  $44\text{ cm}^{-1}$ ) disagreements between our and Ref. [5] data.

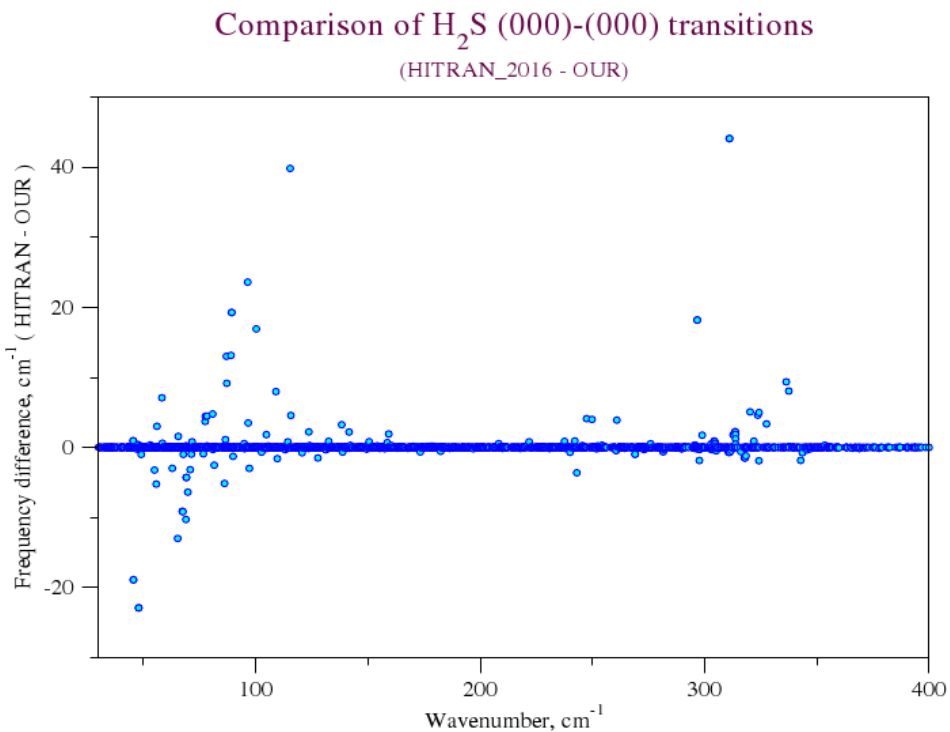


**Fig.1.** Comparison of the (000)-(000) pure rotational transitions of  $\text{H}_2\text{S}$  molecule included into HITRAN 2016 database and those calculated from the parameters presented in Table 1.

To further validate our  $\text{H}_2\text{S}$  calculations based on the Generation function approach, the pure rotational (010)-(010) transitions calculated in this paper were compared with recent variational calculation [7] (see Fig.3). The comparison was limited to  $\text{H}_2\text{S}$  transitions from HITRAN 2016. It is obvious from the figure that our simulation agrees much better with variational calculation than with simulation from Ref. [5] with maximal deviation not exceeding  $0.4\text{ cm}^{-1}$ .

DEVIATIONS OF (010)-(010) H<sub>2</sub>S POSITIONS BETWEEN HITRAN AND OUR CALCULATION

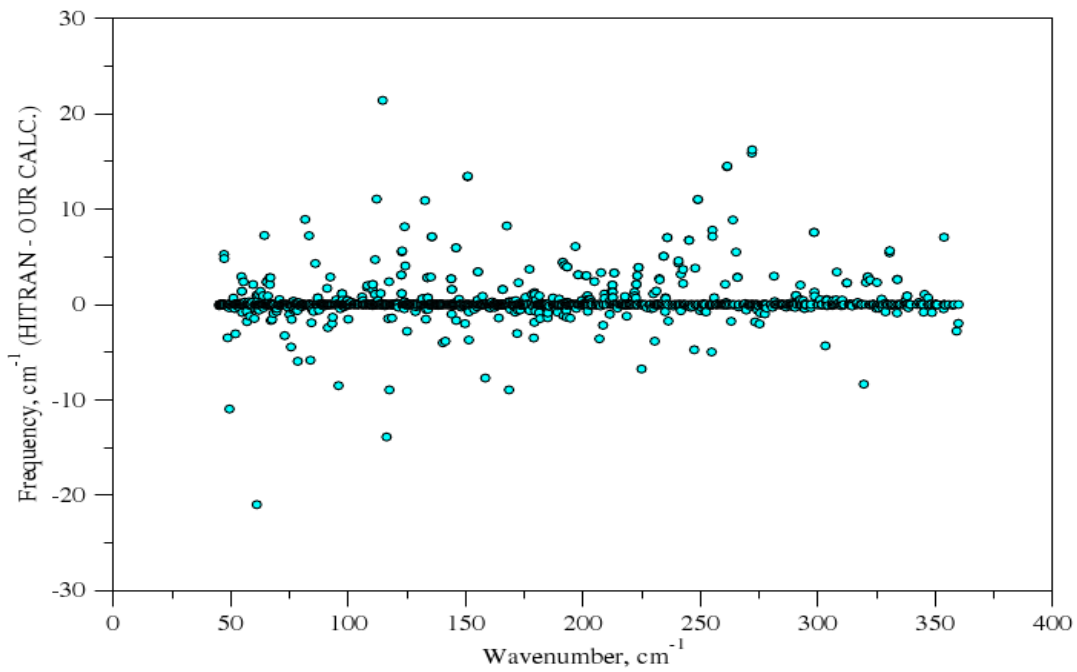


**Fig.2.** Comparison of the (010)-(010) pure rotational transitions of H<sub>2</sub>S molecule included into HITRAN 2016 database and those calculated from the parameters presented in Table 1.

COMPARISON OF OUR AND VARIATIONAL PREDICTED (010)-(010) TRANSITIONS OF H<sub>2</sub>S

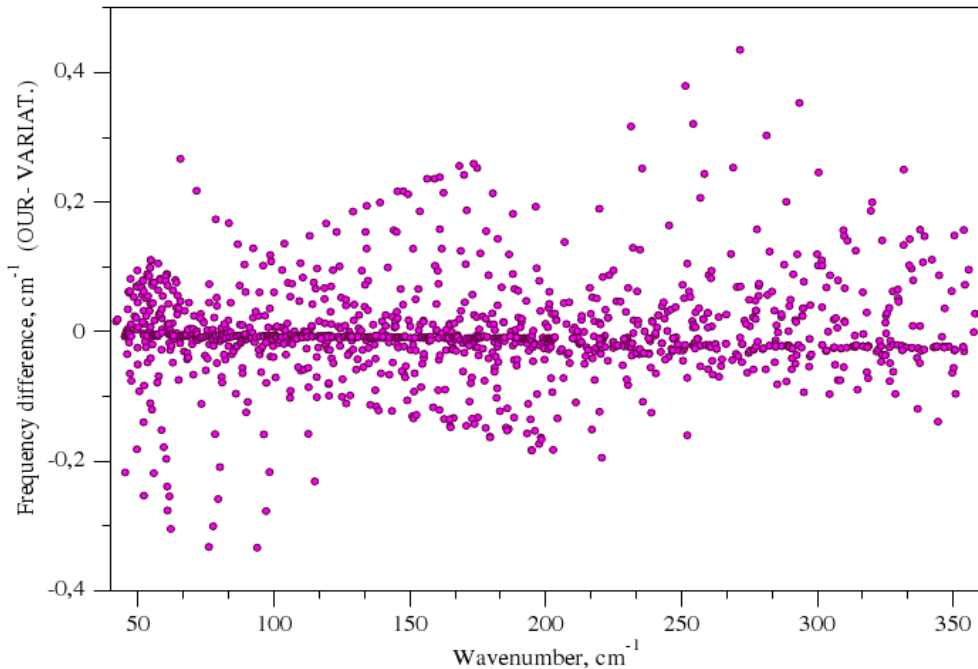


**Fig. 3.** Comparison of the (010)-(010) pure rotational transitions of H<sub>2</sub>S calculated in this paper with recent variational calculation [7].

#### IV. MODELING AND PREDICTING THE H<sub>2</sub>S TRANSITIONS USING EULER SUMMATION METHOD

A set of pure rotational (000)-(000), (010) – (010) H<sub>2</sub>S transitions between 49 and 359 cm<sup>-1</sup> included in HITRAN 2016 database originate from the analysis of the terahertz H<sub>2</sub>S spectrum undertaken in Ref.[5]. In this study newly recorded IR transitions were combined with the MW literature experimental data (1408 in total) and fitted using SPFIT/SPCAT computer code elaborated by H. Pickett [6]. Spectroscopic parameters obtained from the fitting were then used to predict a great number of weak H<sub>2</sub>S transitions missing in experiment. Altogether, 2374 pure rotational transitions in the (000) and (010) vibrational states of H<sub>2</sub>S, mostly weak, were predicted in the considered spectral region, while only 1160 experimental lines were initially assigned.

As it was illustrated in Section III, our calculation of the H<sub>2</sub>S (000) and (010) rotational sublevels considerably disagree with Ref. [5] prediction: of 2374 compared transitions 789 have disagreement in positions between 0.05 and 44 cm<sup>-1</sup> (see also Tables 2-3). To clarify this situation, we made our own fitting of the (000)-(000) experimental H<sub>2</sub>S transitions using SPFIT/SPCAT computer code [6]. The fitting was performed within the Euler method with an RMS of 0.00009 cm<sup>-1</sup> obtained for 1396 transitions by varying 39 parameters. Then the

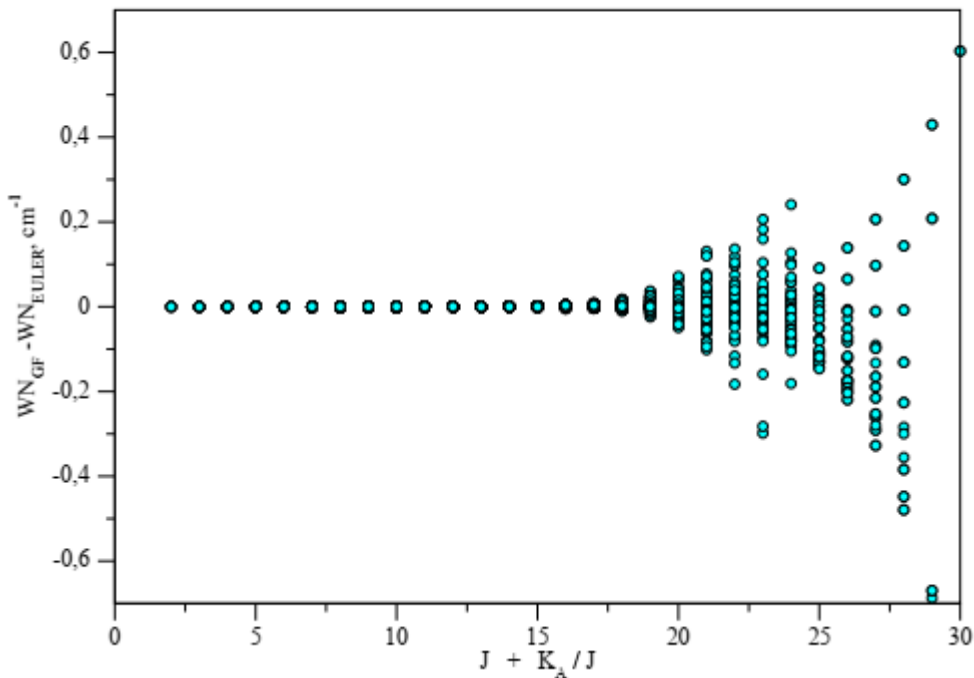


**Fig. 4.** Comparison of the (000)-(000) pure rotational transitions of H<sub>2</sub>S calculated in this paper using Generation functions approach [2,3] and Euler method [6]. Comparison is limited to HITRAN 2016 data set.

parameters obtained were used to predict the same set of weak transitions as in Ref. [5]. Comparison of the set of extrapolated transitions based on GF and Euler approaches is included in Fig. 4. Wavenumbers of both sets of transitions agree within RMS of  $0.08\text{ cm}^{-1}$ , with maximum deviation not exceeding  $0.7\text{ cm}^{-1}$  what is very inspiring provided that a long extrapolation on  $J$  and  $K_a$  rotational quantum numbers was used.

#### IV. CONCLUSION

Recently derived [1] experimental energy levels of the key (000) and (010) vibrational states of  $\text{H}_2\text{S}$  molecule were modeled with the accuracy close to experimental one using the generating function and Euler methods [3,6]. The spectroscopic parameters obtained were used for extrapolating calculations of the (000) and (010) highly excited rotational energy levels and transition wavenumbers. These simulations were compared with the pure rotational (000)-(000) and (010) - (010) transitions from the HITRAN 2016 database based on the original data [5] revealing large - up to  $44\text{ cm}^{-1}$  disagreements.

Comparison of the presently calculated energy levels with recent accurate variational calculations [7] confirmed a high quality of simulation based on GF and Euler methods with maximal deviation not exceeding  $0.4$  and  $0.76\text{ cm}^{-1}$ , respectively. A detailed consideration of the fitting procedure used in [5] allowed us to conclude that, in fact, the Watson - type rotational Hamiltonian with much worse predictive ability was used in [5] instead of Euler approach available in [6], as the main "a" and "b" Euler parameters were set to zero. In addition, it seems also that 12 blended (or misassigned ) less accurate transitions participated in the fitting in [5], what resulted in increase of the number of varied parameters (46 compared to 39 in our study) and further degrading of the prediction accuracy.

Finally, large sets of accurate energy levels for the key (000) and (010) states of  $\text{H}_2\text{S}$  molecule were generated on the base of the GF spectroscopic parameters. These energy levels can be widely used for the  $\text{H}_2\text{S}$  spectra assignment and extrapolation. These data are available from the authors on request.

#### **Acknowledgment**

The work of Naumenko O.V. was supported by the Ministry of Science and Higher Education of the Russian Federation. The study of Polovtseva E.R. and Bykov A.D. was carried out with the financial support of the Russian Foundation for Basic Research (Grant No. 18-02-00462).

### **References:**

- [1] K.L. Chubb, O. Naumenko, et al. Marvel analysis of the measured high-resolution rovibrational spectra of H<sub>2</sub><sup>32</sup>S, JQSRT, 2018, v. 218, pp. 178 - 186.
- [2] S.N. Mikhailenko, Vl.G. Tyuterev, G. Mellau, J. Mol. Spectrosc. 217 (2003) 195-211.
- [3] Vl.G. Tyuterev, J. Mol. Spectrosc. 151 (1992) 97-121.
- [4] Vl.G. Tyuterev, V.I. Starikov, S.A. Tashkun, S.N. Mikhailenko J. Mol. Spectrosc. 170 (1995) 38-58.
- [5] Azzam3. A. A. A. Azzam, S. N. Yurchenko, J. Tennyson, M.-A. Martin, O. Pirali, Terahertz spectroscopy of hydrogen sulfide, J. Quant. Spectrosc. Radiat. Transf. 130 (2013) 341–51.  
doi:10.1016/j.jqsrt.2013.05.035.
- [6] Pickett HM. The fitting and prediction of vibration-rotation spectra with spin interactions. J Mol Spectrosc 1991;148:371–7
- [7]. A. A. A. Azzam, S. N. Yurchenko, J. Tennyson, O. V. Naumenko, ExoMol line lists XVI: A Hot Line List for H<sub>2</sub>S, Mon. Not. R. Astron. Soc. 460 (2016) 4063–4074.

**Table 1.** Parameters of the effective Hamiltonian written through GF for the (000) and (010) vibrational states of the H<sub>2</sub>S molecule.

PAR	VALUE, cm <sup>-1</sup>		PAR	VALUE, cm <sup>-1</sup>	
	(000)	(010)		(000)	(010)
a1	0.27030(240)E-02	0.4832724(900)E-02	g23		-0.3223(750)E-10
a2	0.42914(390)E-05	-0.4665(200)E-05	g33	0.4339(210)E-14	0.2785(200)E-13
a3	-0.516(130)E-09	0.1350(160)E-07	g04	-0.37794(290)E-08	-0.7541(520)E-08
a4	-0.11359(810)E-11	-0.1595(610)E-10	g24	-0.15981(760)E-13	-0.5134(780)E-13
a5		0.6212(700)E-14	g15	0.3262(110)E-13	0.1073(100)E-12
E	0.0	1182.57696000	g06	-0.25538(650)E-13	-0.7037(520)E-13
g10	6.87446394(380)	6.94661604(510)	(B-C)/4	1.07184244(250)	1.13887827(250)
g20	-0.6528257(890)E-03	-0.75491(110)E-03	u10	-0.2956345(520)E-03	-0.3466765(560)E-03
g30	0.274666(780)E-06	0.36387(760)E-06	u20	0.137178(420)E-06	0.181231(390)E-06
g40	-0.16808(280)E-09	-0.1881(170)E-09	u30	-0.8453(140)E-10	-0.93403(860)E-10
g50	0.7714(350)E-13		u40	0.3906(180)E-13	
g01	3.4856935(150)	3.775483(170)	u01	0.132248(150)E-03	0.20853(210)E-04
g11	0.2279979(450)E-02	0.273504(530)E-02	u11	-0.48015(170)E-06	-0.66937(320)E-06
g21	-0.153536(490)E-05	-0.19076(760)E-05	u21	0.44811(760)E-09	0.8589(180)E-09
g31	0.13757(210)E-08	0.2144(410)E-08	u31	-0.2849(110)E-12	-0.9692(350)E-12
g41	-0.8121(310)E-12	-0.1653(770)E-11	u02	0.132058(260)E-05	0.217687(360)E-05
g02	-0.13471(210)E-02		u12	-0.6565(130)E-09	-0.13641(320)E-08
g12	0.65431(330)E-05		u22	0.7936(230)E-12	0.34275(820)E-11
g22	-0.29608(910)E-08		u13	-0.17641(350)E-11	-0.9428(170)E-11
g03	-0.36253(420)E-05	-0.8370(120)E-05	u04	0.26969(360)E-11	0.6965(170)E-11
g13		0.2592(180)E-07			
37 param, 426 levels, RMS=0.000256 cm <sup>-1</sup>			35 param, 301 levels, RMS=0.00020 cm <sup>-1</sup>		
(000)			(010)		

**Table 2.** Comparison of the presently calculated using GF approach (000)-(000) pure rotational transition wavenumbers with those from HITRAN 2016 database for H<sub>2</sub><sup>32</sup>S molecule.<sup>\*)</sup>

Wn, cm <sup>-1</sup>	Intensity	Wn, cm <sup>-1</sup>	E <sub>lower</sub> , cm <sup>-1</sup>	VIB	J K <sub>a</sub> K <sub>c</sub>	VIB	J K <sub>a</sub> K <sub>c</sub>
This work	Cm/mol	HIT - TW			Upper		Lower
50.02800	1.326E-28	-1.018666	4260.7181	000	22 14 8	000	22 13 9
51.16310	7.255E-29	7.083400	4652.9225	000	23 15 8	000	23 14 9
53.01100	1.133E-28	3.007489	4310.7461	000	22 15 7	000	22 14 8
58.18030	9.930E-29	-3.247069	4594.7422	000	23 14 9	000	23 13 10
60.95640	5.766E-29	-5.247698	4704.0856	000	23 16 7	000	23 15 8
63.94320	2.490E-28	1.560563	4196.7749	000	22 13 9	000	22 12 10
64.48180	1.004E-28	-18.926174	4324.0917	000	21 20 1	000	21 19 2
64.48290	3.346E-29	-18.926605	4324.0905	000	21 20 2	000	21 19 3
65.86190	1.005E-28	-2.990330	4363.7571	000	22 16 6	000	22 15 7
68.76130	1.363E-27	-1.001669	4038.7235	000	21 16 5	000	21 15 6
70.03120	3.487E-28	19.263254	4254.0605	000	21 19 2	000	21 18 3
70.04220	1.162E-28	19.263993	4254.0483	000	21 19 3	000	21 18 4
70.81840	9.997E-30	-22.930724	4655.5386	000	22 20 2	000	22 19 3
70.82360	2.999E-29	-22.934187	4655.5328	000	22 20 3	000	22 19 4
72.85110	6.345E-29	23.610855	4765.0420	000	23 17 6	000	23 16 7
73.18720	9.941E-28	4.439430	4107.4848	000	21 17 4	000	21 16 5
73.38850	5.487E-28	-4.304845	4180.6720	000	21 18 3	000	21 17 4
73.48100	1.833E-28	-4.310301	4180.5673	000	21 18 4	000	21 17 5
73.82480	5.967E-28	3.698963	4279.5121	000	22 15 8	000	22 14 9
73.83810	3.364E-28	4.465928	4106.7292	000	21 17 5	000	21 16 6
73.98890	9.021E-29	13.004442	4429.6190	000	22 17 5	000	22 16 6
74.04080	3.716E-28	-3.182941	4353.3369	000	22 16 7	000	22 15 8
75.52250	1.099E-28	39.847444	4580.0103	000	22 19 4	000	22 18 5
75.86450	2.830E-28	13.145652	4427.3777	000	22 17 6	000	22 16 7
76.06710	2.141E-28	4.761906	4518.6751	000	23 13 10	000	23 12 11
76.19660	2.850E-29	-6.404271	4683.0727	000	23 16 8	000	23 15 9
76.45210	4.802E-29	-9.132908	4503.6079	000	22 18 4	000	22 17 5
76.76810	1.450E-28	-9.198275	4503.2422	000	22 18 5	000	22 17 6
77.98330	5.065E-29	9.155393	4605.0894	000	23 15 9	000	23 14 10
78.26270	3.282E-29	-13.014230	4837.8931	000	23 18 5	000	23 17 6
79.24770	1.819E-29	-10.308079	5022.7903	000	24 16 9	000	24 15 10
83.35510	3.687E-29	16.922687	4939.4352	000	24 15 10	000	24 14 11
84.08590	7.657E-29	-2.549055	4521.0035	000	23 14 10	000	23 13 11
85.40940	1.578E-27	1.112189	4116.4738	000	22 13 10	000	22 12 11
91.23680	3.990E-28	-1.288501	4427.4383	000	23 12 11	000	23 11 12
91.27050	5.523E-29	-5.152292	4848.1647	000	24 14 11	000	24 13 12
93.16690	1.409E-28	3.489006	4427.8366	000	23 13 11	000	23 12 12
100.20460	3.366E-29	-3.007418	4746.9425	000	24 12 12	000	24 11 13
101.06070	1.090E-28	7.966880	4747.1040	000	24 13 12	000	24 12 13
102.95310	7.601E-28	1.821074	4324.4852	000	23 11 12	000	23 10 13
111.13720	6.617E-29	4.557913	4635.8053	000	24 11 13	000	24 10 14
111.27710	1.921E-28	-1.610988	4635.8269	000	24 12 13	000	24 11 14
121.47370	3.764E-28	2.200825	4514.3532	000	24 11 14	000	24 10 15
129.24410	9.244E-29	-1.525408	4825.8385	000	25 10 15	000	25 9 16
135.10280	1.463E-28	3.234916	4045.5692	000	21 17 4	000	20 20 1
139.42100	1.904E-28	2.192439	4686.4175	000	25 9 16	000	25 8 17
157.38230	9.980E-29	1.911638	4840.9796	000	26 9 18	000	26 8 19
243.34910	2.250E-28	4.106277	3937.3229	000	21 17 4	000	20 18 3
245.85210	6.097E-28	3.986492	4107.4848	000	22 15 8	000	21 16 5
246.70570	5.272E-28	-3.635878	4180.6720	000	22 16 7	000	21 17 4
257.02790	2.702E-28	3.889352	4106.7292	000	22 15 7	000	21 16 6
266.95930	1.161E-27	44.126709	4388.5735	000	22 19 4	000	21 20 1
266.96520	3.869E-28	44.123040	4388.5734	000	22 19 3	000	21 20 2

<b>Wn, cm<sup>-1</sup></b>	<b>Intensity</b>	<b>Wn, cm<sup>-1</sup></b>	<b>E<sub>lower, cm<sup>-1</sup></sub></b>	<b>VIB</b>	<b>J K<sub>a</sub> K<sub>c</sub></b>	<b>VIB</b>	<b>J K<sub>a</sub> K<sub>c</sub></b>
<b>This work</b>	<b>Cm/mol</b>	<b>HIT - TW</b>			<b>Upper</b>		<b>Lower</b>
278.52130	1.028E-27	18.193729	4045.5692	000	21 19 3	000	20 20 0
278.52250	3.084E-27	18.193324	4045.5692	000	21 19 2	000	20 20 1
297.20330	2.806E-27	1.735027	3963.5148	000	22 13 9	000	21 14 8
299.58560	1.007E-27	-1.877097	4353.3369	000	23 14 9	000	22 15 8
310.96450	1.053E-26	1.783344	4116.4738	000	23 11 12	000	22 12 11
311.34170	4.756E-27	2.225279	4324.4852	000	24 11 14	000	23 10 13
311.48530	2.243E-27	2.229811	4514.3532	000	25 9 16	000	24 10 15
311.94440	1.128E-27	1.849893	4686.4175	000	26 9 18	000	25 8 17
312.57970	6.071E-28	1.219128	4840.9796	000	27 7 20	000	26 8 19
315.23010	2.576E-27	5.068935	4279.5121	000	23 13 10	000	22 14 9
319.10590	8.695E-28	4.591774	4427.8366	000	24 11 13	000	23 12 12
319.25570	1.161E-27	-1.496422	4635.8269	000	25 10 15	000	24 11 14
319.28560	3.869E-28	4.967560	4635.8053	000	25 11 15	000	24 10 14
319.57350	5.398E-28	-1.526056	4825.8385	000	26 10 17	000	25 9 16
319.66570	2.667E-27	-1.206783	4427.4383	000	24 12 13	000	23 11 12
324.22860	2.135E-27	3.344932	4196.7749	000	23 13 11	000	22 12 10
326.14360	4.914E-28	-1.904650	4521.0035	000	24 12 12	000	23 13 11
327.03100	6.079E-28	9.361014	4747.1040	000	25 11 14	000	24 12 13
329.48960	1.475E-27	8.048597	4518.6751	000	24 13 12	000	23 12 11
344.69300	9.214E-28	-1.865600	4594.7422	000	24 14 11	000	23 13 10

<sup>\*)</sup> Only transitions with  $\Delta = | \mathbf{V}_{\text{HIT}} - \mathbf{V}_{\text{TW}} | \geq 1 \text{ cm}^{-1}$  are included.

**Table 3.** Comparison of the presently calculated using GF approach (010)-(010) pure rotational transition wavenumbers with those from HITRAN 2016 database for H<sub>2</sub><sup>32</sup>S molecule .<sup>\*)</sup>

Wn, cm <sup>-1</sup>	Intensity	Wn, cm <sup>-1</sup>	E <sub>lower</sub> , cm <sup>-1</sup>	VIB	J K <sub>a</sub> K <sub>c</sub>	VIB	J K <sub>a</sub> K <sub>c</sub>
This work	Cm/mol	HIT - TW		Upper		Lower	
41.87520	7.048E-31	5.256199	3720.5943	010	18 6 12	010	17 9 9
42.39200	2.155E-30	4.818959	3720.0792	010	18 7 12	010	17 8 9
51.61560	2.029E-29	2.925450	3481.5722	010	17 6 11	010	16 9 8
52.19330	1.948E-28	-3.501124	4123.3399	010	18 11 7	010	18 10 8
53.03120	7.204E-30	2.385056	3480.1619	010	17 7 11	010	16 8 8
53.33150	3.420E-29	1.378892	3369.4762	010	17 5 12	010	18 4 15
53.33180	1.140E-29	1.379523	3369.4762	010	17 6 12	010	18 3 15
55.08190	6.184E-32	-3.073612	3533.1931	010	16 10 6	010	17 7 11
57.05730	3.435E-31	7.244876	3997.3381	010	18 10 9	010	17 13 4
57.37690	1.467E-27	2.101508	3939.9612	010	17 13 4	010	17 12 5
58.68660	7.757E-32	-1.797756	3312.5656	010	15 11 5	010	16 6 10
59.43230	4.834E-31	-1.243890	3491.2620	010	16 10 7	010	15 13 2
60.39700	1.125E-31	-10.959077	3870.8149	010	17 12 6	010	18 7 11
60.89330	4.051E-27	1.019228	3430.2842	010	15 13 3	010	15 12 4
61.25450	4.259E-29	1.391617	3251.3111	010	16 6 10	010	15 9 7
61.51670	2.344E-31	-1.461883	3551.8042	010	16 11 6	010	15 14 1
62.96820	1.165E-29	2.358405	3579.9717	010	18 5 13	010	19 4 16
62.96830	3.497E-29	2.358671	3579.9717	010	18 6 13	010	19 3 16
63.70070	9.988E-28	2.800296	3737.6323	010	16 14 2	010	16 13 3
64.07650	3.025E-27	2.818147	3737.2169	010	16 14 3	010	16 13 4
64.54440	5.987E-28	2.095163	3931.2119	010	17 13 5	010	17 12 6
68.76640	1.362E-27	-1.683496	3798.0774	010	17 11 7	010	17 10 8
69.18270	8.916E-28	-1.575520	4130.6283	010	18 12 7	010	18 11 8
72.73750	1.138E-30	8.927057	3798.0774	010	18 7 11	010	17 10 8
76.03800	2.322E-31	-1.051570	3551.7984	010	16 11 5	010	15 14 2
76.13770	3.929E-30	7.215534	3794.6968	010	18 8 11	010	17 9 8
76.23290	1.439E-27	-3.263290	4054.3954	010	18 11 8	010	18 10 9
77.48310	2.311E-27	-1.568694	3720.5943	010	17 10 8	010	17 9 9
80.13310	7.069E-31	-4.460848	3533.1878	010	16 11 6	010	17 6 11
81.68180	5.039E-29	4.304797	3550.6943	010	17 7 10	010	16 10 7
82.08480	5.151E-31	-20.994947	4117.7262	010	18 12 7	010	19 7 12
84.48940	1.563E-28	-5.954743	4319.1832	010	19 11 9	010	19 10 10
86.29250	2.576E-27	-1.922226	3968.1029	010	18 10 9	010	18 9 10
89.32240	1.036E-28	1.699229	3313.0649	010	16 7 9	010	15 10 6
89.52570	2.320E-29	2.878604	3542.9093	010	17 8 10	010	16 9 7
89.76080	9.232E-31	-5.847619	3762.4712	010	17 10 7	010	18 7 12
93.28920	1.384E-30	21.410597	4130.6283	010	19 8 11	010	18 11 8
93.80470	4.966E-31	-2.435828	3801.2934	010	17 11 6	010	16 14 3
94.74240	8.980E-28	-1.336343	4223.9175	010	19 9 10	010	19 8 11
95.20050	2.961E-28	-2.007462	4223.9827	010	19 10 10	010	19 9 11
96.28120	2.086E-28	1.136105	3415.7675	010	18 5 14	010	19 2 17
96.28120	6.955E-29	1.136261	3415.7675	010	18 4 14	010	19 3 17
101.07510	1.608E-30	11.053448	3866.8438	010	18 8 10	010	17 11 7
101.59600	3.678E-31	-1.546939	3211.4689	010	15 10 6	010	16 5 11
104.37430	4.926E-31	-8.508389	3762.4695	010	17 11 7	010	18 6 12
106.19130	1.729E-27	1.991170	4117.7262	010	19 8 11	010	19 7 12
106.25000	5.758E-28	1.797467	4117.7327	010	19 9 11	010	19 8 12
106.75830	8.643E-29	4.706817	3613.3209	010	17 8 9	010	16 11 6
108.34540	2.991E-27	2.102164	3762.4695	010	18 7 11	010	18 6 12
108.36330	8.972E-27	2.103314	3762.4712	010	18 8 11	010	18 7 12
108.90970	1.370E-28	1.529058	3371.2522	010	16 8 8	010	15 11 5
110.38010	4.096E-26	1.058887	3422.8077	010	17 6 11	010	17 5 12

<b>Wn, cm<sup>-1</sup></b>	<b>Intensity</b>	<b>Wn, cm<sup>-1</sup></b>	<b>E<sub>lower</sub>, cm<sup>-1</sup></b>	<b>VIB</b>	<b>J K<sub>a</sub> K<sub>c</sub></b>	<b>VIB</b>	<b>J K<sub>a</sub> K<sub>c</sub></b>
<b>This work</b>	<b>Cm/mol</b>	<b>HIT - TW</b>		<b>Upper</b>		<b>Lower</b>	
110.38510	1.365E-26	1.059470	3422.8080	010	17 7 11	010	17 6 12
112.62510	5.609E-29	1.166412	3430.2842	010	16 9 7	010	15 12 4
115.01510	1.121E-29	2.393971	3737.2169	010	17 10 7	010	16 13 4
115.87090	1.098E-29	8.156679	3852.2320	010	18 9 10	010	17 10 7
117.33620	3.391E-27	5.522567	4000.3900	010	19 7 12	010	19 6 13
117.34210	1.131E-27	5.625303	4000.3906	010	19 8 12	010	19 7 13
118.56000	5.093E-31	-1.484741	3312.5826	010	15 12 3	010	16 7 10
119.52960	5.615E-27	3.104608	3642.9399	010	18 6 12	010	18 5 13
119.53120	1.685E-26	3.106681	3642.9400	010	18 7 12	010	18 6 13
120.10130	6.171E-31	-1.419930	3422.8080	010	16 9 7	010	17 6 12
120.26050	6.781E-29	4.049140	3674.4363	010	17 9 8	010	16 12 5
121.66240	7.485E-26	1.146262	3301.1453	010	17 5 12	010	17 4 13
121.66270	2.495E-26	1.146891	3301.1453	010	17 6 12	010	17 5 13
121.82700	1.590E-30	10.900042	3931.2119	010	18 9 9	010	17 12 6
126.50360	3.708E-31	-8.961356	3870.8345	010	17 13 4	010	18 8 11
127.88660	2.308E-30	-2.801562	3422.8077	010	16 10 7	010	17 5 12
128.55370	6.594E-27	7.117474	3871.8363	010	19 6 13	010	19 5 14
128.55420	2.198E-27	7.085310	3871.8364	010	19 7 13	010	19 6 14
130.23830	2.189E-30	-13.896860	4000.3900	010	18 11 8	010	19 6 13
130.89120	1.049E-26	2.809550	3512.0487	010	18 5 13	010	18 4 14
130.89130	3.147E-26	2.809425	3512.0487	010	18 6 13	010	18 5 14
132.31930	9.645E-29	2.879252	3588.2750	010	17 9 9	010	16 10 6
134.63100	5.193E-28	-1.540521	3542.9093	010	16 12 4	010	16 9 7
137.45630	7.925E-28	13.463488	4109.4637	010	20 6 14	010	20 5 15
137.45650	2.377E-27	13.398913	4109.4637	010	20 7 14	010	20 6 15
140.01410	1.257E-26	5.938003	3731.8222	010	19 5 14	010	19 4 15
140.01420	4.189E-27	5.946491	3731.8222	010	19 6 14	010	19 5 15
141.19730	2.818E-28	2.698775	3438.7744	010	19 4 16	010	20 1 19
141.19730	8.454E-28	2.698214	3438.7744	010	19 3 16	010	20 2 19
142.57250	1.938E-26	1.586673	3369.4762	010	18 4 14	010	18 3 15
142.57250	5.815E-26	1.586601	3369.4762	010	18 5 14	010	18 4 15
144.34720	2.557E-31	-4.019921	3533.1931	010	16 12 4	010	17 7 11
145.10610	3.030E-28	-1.010422	3852.2320	010	17 13 4	010	17 10 7
145.26440	6.226E-28	-3.847330	3794.6968	010	17 12 5	010	17 9 8
147.67450	5.864E-28	-1.668324	3480.1619	010	16 11 5	010	16 8 8
151.75680	3.743E-30	-2.005539	3642.9400	010	17 9 8	010	18 6 13
151.85050	2.347E-26	3.430278	3579.9717	010	19 4 15	010	19 3 16
151.85050	7.823E-27	3.427918	3579.9717	010	19 5 15	010	19 4 16
155.13750	1.312E-30	-3.720284	3642.9399	010	17 10 8	010	18 5 13
159.29730	6.792E-29	8.246105	3895.0981	010	18 10 9	010	17 11 6
164.20420	1.428E-26	1.587406	3415.7675	010	19 4 16	010	19 3 17
164.20420	4.282E-26	1.586859	3415.7675	010	19 3 16	010	19 2 17
165.55210	1.028E-30	-1.418050	3211.4701	010	15 11 4	010	16 6 11
166.12100	6.700E-29	-7.711310	4053.0389	010	18 12 6	010	18 9 9
170.24100	4.427E-28	2.290327	3627.8364	010	17 10 8	010	16 11 5
173.49660	1.487E-29	3.700608	3627.8364	010	16 14 2	010	16 11 5
175.01890	4.447E-28	-3.040313	3720.0792	010	17 11 6	010	17 8 9
177.25280	2.437E-26	1.054645	3238.5147	010	19 3 17	010	19 2 18
177.25280	7.311E-26	1.054742	3238.5147	010	19 2 17	010	19 1 18
177.49000	1.017E-30	-8.959550	3762.4712	010	17 12 5	010	18 7 12
178.11260	8.713E-29	1.263912	3313.0649	010	15 13 3	010	15 10 6
178.43250	1.823E-27	1.054464	3237.3350	010	19 2 17	010	20 1 20
178.43250	6.077E-28	1.054370	3237.3350	010	19 3 17	010	20 0 20
181.20250	1.727E-30	-1.868267	3871.8364	010	18 9 9	010	19 6 14
182.55910	4.976E-30	-3.516096	3871.8363	010	18 10 9	010	19 5 14
183.17430	5.095E-27	-1.479874	3491.2620	010	16 12 5	010	15 13 2
186.36280	1.848E-27	-1.393337	3491.1775	010	16 12 4	010	15 13 3

<b>Wn, cm<sup>-1</sup></b>	<b>Intensity</b>	<b>Wn, cm<sup>-1</sup></b>	<b>E<sub>lower</sub>, cm<sup>-1</sup></b>	<b>VIB</b>	<b>J K<sub>a</sub> K<sub>c</sub></b>	<b>VIB</b>	<b>J K<sub>a</sub> K<sub>c</sub></b>
<b>This work</b>	<b>Cm/mol</b>	<b>HIT - TW</b>		<b>Upper</b>		<b>Lower</b>	
186.99780	2.805E-26	4.421033	3438.7744	010	20 3 18	010	20 2 19
186.99780	9.349E-27	4.421684	3438.7744	010	20 2 18	010	20 1 19
187.97250	2.453E-29	4.102332	3613.3209	010	16 14 3	010	16 11 6
189.33540	1.596E-27	3.941406	3436.4368	010	20 3 18	010	21 0 21
189.33540	5.321E-28	3.941949	3436.4368	010	20 2 18	010	21 1 21
190.66710	2.927E-28	6.083093	3939.9612	010	18 11 8	010	17 12 5
192.86410	4.617E-28	-1.170982	3481.5722	010	16 12 5	010	16 9 8
194.42330	3.768E-28	-1.346770	3801.3330	010	17 13 5	010	16 14 2
194.83190	1.412E-27	3.117200	3606.4615	010	16 14 3	010	15 15 0
194.87180	4.714E-28	3.124228	3606.4612	010	16 14 2	010	15 15 1
196.04470	1.180E-27	-1.434598	3801.2934	010	17 13 4	010	16 14 3
198.27200	3.921E-28	3.020603	3863.9079	010	17 14 4	010	16 15 1
198.47230	1.182E-27	3.022034	3863.9052	010	17 14 3	010	16 15 2
202.47290	3.388E-28	2.406065	3997.3381	010	18 12 7	010	17 13 4
204.35600	3.213E-28	3.340924	4062.3775	010	18 13 6	010	17 14 3
208.03050	6.921E-30	1.097147	3512.0487	010	17 8 9	010	18 5 14
210.00470	1.157E-25	3.310314	3415.7675	010	20 2 18	010	19 3 17
210.00470	3.472E-25	3.309678	3415.7675	010	20 3 18	010	19 2 17
210.49550	1.251E-25	2.037818	3369.4762	010	19 4 16	010	18 3 15
210.49550	3.752E-25	2.037355	3369.4762	010	19 3 16	010	18 4 15
210.61760	7.876E-29	-3.600714	3720.5943	010	17 12 6	010	17 9 9
210.75620	6.566E-28	-2.177310	3402.5647	010	16 11 6	010	16 8 9
210.90340	1.479E-25	1.354042	3301.1453	010	18 4 14	010	17 5 13
210.90340	4.438E-25	1.353972	3301.1453	010	18 5 14	010	17 4 13
211.33760	5.738E-25	1.282397	3211.4701	010	17 5 12	010	16 6 11
211.33910	1.913E-25	1.284087	3211.4689	010	17 6 12	010	16 5 11
212.40140	5.666E-28	-1.017239	3100.6635	010	15 10 6	010	15 7 9
219.77350	1.849E-25	3.881032	3512.0487	010	19 4 15	010	18 5 14
219.77350	6.163E-26	3.879063	3512.0487	010	19 5 15	010	18 4 14
219.85590	3.296E-28	-1.227039	3632.3761	010	17 10 7	010	17 7 10
220.13190	7.972E-26	3.016700	3422.8080	010	18 5 13	010	17 6 12
220.13230	2.392E-25	3.017134	3422.8077	010	18 6 13	010	17 5 12
220.60520	3.354E-25	2.119548	3312.5826	010	17 6 11	010	16 7 10
220.62750	1.118E-25	2.116358	3312.5656	010	17 7 11	010	16 6 10
220.66180	7.191E-27	1.302089	3674.4363	010	17 11 6	010	16 12 5
228.85080	1.009E-25	1.122918	3251.3111	010	16 8 8	010	15 9 7
228.89630	9.490E-26	7.009610	3642.9400	010	19 5 14	010	18 6 13
228.89650	3.163E-26	7.016004	3642.9399	010	19 6 14	010	18 5 13
229.27640	4.454E-26	5.061838	3533.1931	010	18 6 12	010	17 7 11
229.28340	1.337E-25	5.064928	3533.1878	010	18 7 12	010	17 6 11
229.81140	2.018E-25	2.727885	3402.5647	010	17 7 10	010	16 8 9
229.84440	4.998E-26	1.411096	3313.0649	010	16 9 7	010	15 10 6
230.04770	6.733E-26	2.590471	3402.3873	010	17 8 10	010	16 7 9
231.70810	1.509E-28	-6.761036	3968.1029	010	18 12 7	010	18 9 10
234.40880	1.044E-28	-3.845754	3632.4350	010	17 11 7	010	17 8 10
236.09670	2.668E-30	4.580155	3731.8222	010	18 8 10	010	19 5 15
236.28070	8.122E-30	4.344133	3731.8222	010	18 9 10	010	19 4 15
237.91880	5.030E-26	11.020403	3762.4712	010	19 6 13	010	18 7 12
237.92110	1.677E-26	10.996707	3762.4695	010	19 7 13	010	18 6 12
238.11170	6.795E-28	-1.740902	3312.5826	010	16 10 7	010	16 7 10
238.37990	2.557E-26	6.764799	3632.4350	010	18 7 11	010	17 8 10
238.45840	7.673E-26	6.723894	3632.3761	010	18 8 11	010	17 7 10
238.50700	1.231E-25	3.171420	3481.5722	010	17 8 9	010	16 9 8
238.91110	2.740E-26	3.678156	3613.3209	010	17 10 7	010	16 11 6
240.43240	4.151E-26	2.190696	3480.1619	010	17 9 9	010	16 8 8
244.00250	6.995E-26	3.813157	3550.6943	010	17 9 8	010	16 10 7
246.89170	2.716E-26	14.439656	3870.8345	010	19 7 12	010	18 8 11

<b>Wn, cm<sup>-1</sup></b>	<b>Intensity</b>	<b>Wn, cm<sup>-1</sup></b>	<b>E<sub>lower</sub>, cm<sup>-1</sup></b>	<b>VIB</b>	<b>J K<sub>a</sub> K<sub>c</sub></b>	<b>VIB</b>	<b>J K<sub>a</sub> K<sub>c</sub></b>
<b>This work</b>	<b>Cm/mol</b>	<b>HIT - TW</b>		<b>Upper</b>		<b>Lower</b>	
246.91780	9.055E-27	14.519846	3870.8149	010	19 8 12	010	18 7 11
247.32460	1.497E-26	7.801258	3720.5943	010	18 8 10	010	17 9 9
248.02370	4.480E-26	7.128000	3720.0792	010	18 9 10	010	17 8 9
252.15810	1.050E-30	-4.752590	3642.9400	010	17 11 6	010	18 6 13
254.96150	8.719E-27	8.868022	3798.0774	010	18 9 9	010	17 10 8
255.81460	1.472E-26	16.225081	3968.1029	010	19 8 11	010	18 9 10
256.06380	4.913E-27	15.874417	3967.9189	010	19 9 11	010	18 8 10
258.42370	1.400E-30	2.126627	3542.9093	010	16 14 2	010	16 9 7
259.69860	2.667E-26	5.499054	3794.6968	010	18 10 9	010	17 9 8
259.79380	2.000E-28	-4.979771	3870.8345	010	18 11 8	010	18 8 11
262.89990	7.841E-30	2.882127	3369.4762	010	17 7 10	010	18 4 15
262.95880	2.614E-30	2.838196	3369.4762	010	17 8 10	010	18 3 15
264.88430	1.169E-28	-1.763054	3533.1931	010	17 10 8	010	17 7 11
275.15300	3.665E-30	-1.828654	3402.3873	010	16 12 4	010	16 7 9
277.25890	3.747E-30	-2.039083	3720.0792	010	17 13 4	010	17 8 9
278.39630	1.783E-26	2.971163	3852.2320	010	18 11 8	010	17 10 7
290.56940	8.419E-29	2.043129	3762.4695	010	18 9 9	010	18 6 12
290.84320	2.661E-30	7.565177	3579.9717	010	18 7 11	010	19 4 16
290.86280	7.921E-30	7.568666	3579.9717	010	18 8 11	010	19 3 16
297.27150	3.872E-28	1.304856	3422.8077	010	17 8 9	010	17 5 12
304.71290	1.724E-26	3.407295	3895.0981	010	18 12 7	010	17 11 6
307.58510	7.970E-30	-4.338969	3632.3761	010	17 12 5	010	17 7 10
310.03140	2.666E-25	2.258043	3491.2620	010	16 14 3	010	15 13 2
310.15550	8.892E-26	2.273811	3491.1775	010	16 14 2	010	15 13 3
318.21600	2.881E-26	2.320010	3677.5403	010	17 13 5	010	16 12 4
318.41960	4.979E-30	2.900155	3214.7682	010	17 6 11	010	18 3 16
318.42490	1.660E-30	2.901368	3214.7682	010	17 7 11	010	18 2 16
319.72120	1.391E-29	2.566934	3481.5722	010	16 14 3	010	16 9 8
322.90180	8.966E-26	2.303318	3674.4363	010	17 13 4	010	16 12 5
324.97900	1.084E-28	5.649668	3642.9399	010	18 8 10	010	18 5 13
325.16290	3.245E-28	5.415740	3642.9400	010	18 9 10	010	18 6 13
327.97470	1.370E-30	-8.354906	3871.8363	010	18 12 7	010	19 5 14
331.23080	4.371E-28	2.649497	3301.1453	010	17 7 10	010	17 4 13
331.28970	1.456E-28	2.605565	3301.1453	010	17 8 10	010	17 5 13
344.40380	6.102E-26	1.066106	3550.6943	010	17 11 6	010	16 10 7
346.70370	3.404E-30	7.052211	3415.7675	010	18 7 12	010	19 2 17
361.85370	4.796E-30	-1.976885	3312.5826	010	16 12 5	010	16 7 10
361.91030	1.847E-30	-2.794344	3533.1878	010	17 11 6	010	17 6 11

<sup>\*)</sup> Only transitions with  $\Delta = | \mathbf{V}_{\text{HIT}} - \mathbf{V}_{\text{TW}} | \geq 1 \text{ cm}^{-1}$  are included.